*Nanochem Res 7(1): 44-52, Winter and Spring 2022*

RESEARCH PAPER

# Synthesis of Thiazole-2(3H)-thiones as Antimicrobial Agents Promoted by $H_3PW_{12}O_{40}$-amino-functionalized $CdFe_{12}O_{19}@SiO_2$ Nanocomposite

***Hossein Shahbazi-Alavi*** [1,*], ***Javad Safaei-Ghomi*** [2]

[1] *Young Researchers and Elite Club, Kashan Branch, Islamic Azad University, Kashan, Iran*

[2] *Department of Organic Chemistry, Faculty of Chemistry, University of Kashan, Kashan, Iran*

**ARTICLE INFO**

***Article History:***
*Received 04 February 2022*
*Accepted 23 April 2022*
*Published 1 May 2022*

***Keywords:***
*Thiazole-2(3H)-thione*
*Nanocomposites*
*Nanocatalyst*
*Antimicrobial*
*one-pot*

**ABSTRACT**

$H_3PW_{12}O_{40}$-amino-functionalized $CdFe_{12}O_{19}@SiO_2$ nanocomposite has been utilized as an effective nanocatalyst for the preparation of thiazole-2(3H)-thiones by three-component reactions of $CS_2$, 2-bromoacetophenone or 2-bromo-1-(4-methoxyphenyl) ethenone, and a primary amine in ethanol. $H_3PW_{12}O_{40}$-amino-functionalized $CdFe_{12}O_{19}@SiO_2$ nanocomposites have been identified by powder X-ray diffraction (XRD), scanning electronic microscopy (SEM), energy dispersive X-ray spectroscopy (EDS), vibrating sample magnetometer (VSM), thermal gravimetric analysis (TGA), and Fourier transform infrared (FT-IR) spectroscopy. The compounds **4b** (3-(3,4-dichlorobenzyl)-4-phenyl-1,3-thiazole-2(3H)-thione), **4e** (3-(4-Fluorobenzyl)-4-phenyl-1,3-thiazole-2(3H)-thione), **4f** (3-(2-Methoxybenzyl)-4-phenyl-1,3-thiazole-2(3H)-thione), and **4j** (3-(2-Methoxybenzyl)-4-(4-methoxyphenyl)-1,3-thiazole-2(3H)-thione) have moderate growth inhibitory effects on Gram positive bacteria (*Staphylococcus aureus, Bacillus subtilis*; and *Staphylococcus epidermidis*). In addition, the compound **4b** has moderate growth inhibitory effects on fungi. The salient features of this protocol include great yields in concise times, retrievability of the nanocatalyst, little nanocatalyst loading, and antibacterial activities for four compounds.

**How to cite this article**
*Shahbazi-Alavi H., Safaei-Ghomi J. Synthesis of Thiazole-2(3H)-thiones as Antimicrobial Agents Promoted by $H_3PW_{12}O_{40}$-amino-functionalized $CdFe_{12}O_{19}@SiO_2$ Nanocomposite. Nanochem Res, 2022; 7(1):44-52. DOI: 10.22036/ncr.2022.01.007*

## INTRODUCTION

Thiazoles show anticancer [1], antifungal [2], anti-inflammatory [3], anti-Candida [4], and antibacterial properties [5]. Some other examples of thiazoles like prominent drug molecules such as Pramipexole [6], Tiazofurin [7], Ritonavir [8], and Nizatidine [9] are applied for their high bioavailability, prolonged effects, and a slower onset (Scheme 1). These properties make thiazoles appealing goals in organic synthesis. Past reports on the synthesis of 1,3-thiazole derivatives have mentioned catalysts such as 1,8-diazabicyclo[5.4.0]undec-7-ene [10], perchloric acid-$SiO_2$ [11], $Bi(SCH_2COOH)_3$ [12], triethylammonium hydrogen sulfate [13], and ytterbium(III) triflate [14]. Whereas these ways have substantial negative aspects including high reaction times, low yields, unwanted reaction conditions, and the use of costly and toxic catalysts. Appling environmental and green nanocatalysts, which can be quickly recycled at the end of reactions, has received great attention in recent years [15,16]. Nanocomposites have appeared as a proper group of heterogeneous catalysts due to their numerous usages in synthesis and catalysis [17-18]. Since these nanocomposites are often retrieved easily by simple workup, which prevents organic products from contamination, they may be investigated as promising, safe, reusable, and greener catalysts compared to traditional ones [19-23]. Newly, magnetic nanocomposite particles (MNPs) have been utilized to immobilize organocatalysts, polymers,

* Corresponding Author Email: *hosseinshahbazi99@yahoo.com*

enzymes, and transition metal catalysts [24-26]. Different types of magnetic nanocatalysts have been improved to efficiently promote multi-component reactions for the synthesis of medicinal compounds [27-28]. These nanocomposites are recyclable and can be retrieved in consecutive trials without significantly decreasing their catalytic attributes [29-30]. The heteropolyacids are extensively applied as homogeneous and heterogeneous catalysts [31-32]. In this work, $H_3PW_{12}O_{40}$–amino was tethered to magnetic nanocomposite particles for preparing a reusable magnetic catalyst. Furthermore, we considered a useful way for the synthesis of thiazole-2(3H)-thiones as antimicrobial agents by three-component reactions of $CS_2$, 2-bromoacetophenone or 2-bromo-1-(4-methoxyphenyl)ethanone and a primary amine (Scheme 2).

## EXPERIMENTAL SECTION

*Chemicals and apparatus*

All materials were commercially purchased from Merck and Sigma-Aldrich. Powder X-ray diffraction (XRD) was registered on a Philips diffractometer of X'pert Company with monochromatized Cu Kα radiation (λ = 1.5406 Å). The microscopic morphology of the nanocatalyst was recorded by SEM (MIRA3). The thermogravimetric analysis (TGA) curves were investigated using a V5.1A Dupont 2000. The magnetic measurement of samples was studied in a vibrating sample magnetometer (VSM) (Kashan, Iran: Kavir Co). Fourier transform infrared measurements were conducted on Magna 550 instrument by using potassium bromide (KBr) plates. NMR spectra were recorded on a Bruker 400 MHz spectrometer with DMSO-$d_6$ as the solvent and TMS as internal standard.

*Preparation of $CdFe_{12}O_{19}$ nanoparticle:*

The $CdFe_{12}O_{19}$ nanocomposites were synthesized using sol-gel auto-combustion path of a solution of $Cd(NO_3)_2.4H_2O$ and $Fe(NO_3)_3.9H_2O$ with the molar ratio of 1 to 12 for Cd:Fe. Initially, cadmium nitrate tetrahydrate was solved in distilled water. Afterwards, pomegranate juice (15 mL) was

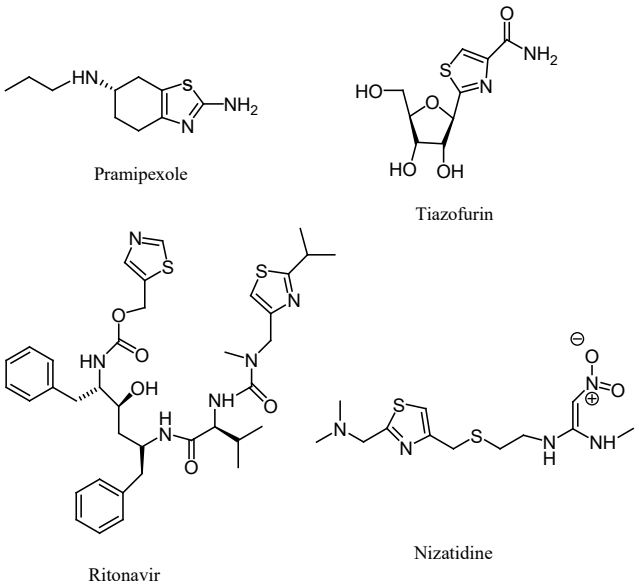


Scheme 1. Drugs with thiazole structure

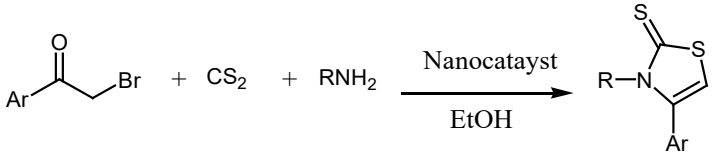


Scheme 2. Synthesis of thiazole-2(3H)-thione by nanocatalyst

added into the solution drop-wise under strong magnetic stirring for 30 min. Next, an aqueous solution containing Iron (III) nitrate nonahydrate was added to the solution and heated at 90 °C for 60 min to form a viscous gel. The gel was dried in an oven at 100 °C. The final residue was calcined at 800 °C for 120 min [33-34]. Meanwhile, the final remnants were powdered by mortar.

*Preparation of $CdFe_{12}O_{19}@SiO_2$ nanocomposites*

The nano-$CdFe_{12}O_{19}$ powder (1g) was dispersed in 20 mL ethanol in ultrasonic bath and sonicated for 50 min at 40 °C. A concentrated ammonia solution (1.5 mL) was added under magnetic stirring at 40 °C for 30 min. Then, tetraethyl orthosilicate (TEOS, 1.0 mL) was added to the solution and stirred at 40 °C for 24 h. $CdFe_{12}O_{19}@SiO_2$ nanocomposites were collected using an external magnet and washed with ethanol and dried in a vacuum for 24 h.

*Preparation of amino-functionalized $CdFe_{12}O_{19}@SiO_2$ nanocomposites*

$CdFe_{12}O_{19}@SiO_2$ (1 g) was added to the solution of 3-aminopropyltriethoxysilane (APTES) (2 mmol, 0.44 g) in dry toluene (20 mL) and refluxed for 20 h. Finally, amino-functionalized $CdFe_{12}O_{19}@SiO_2$ nanocomposites were collected by a magnet, washed with double-distilled water and anhydrous ethanol, and dried at 80 °C for 8 h.

*Preparation of $H_3PW_{12}O_{40}$-amino-functionalized $CdFe_{12}O_{19}@SiO_2$ nanocomposites*

Amino-functionalized $CdFe_{12}O_{19}@SiO_2$ (1 g) was added to the solution of 0.3 g of $H_3PW_{12}O_{40}$ in methanol (25 mL) and the reaction mixture was refluxed for 6 h. Finally, $H_3PW_{12}O_{40}$-amino-functionalized $CdFe_{12}O_{19}@SiO_2$ nanocomposites were collected by a magnet, rinsed with methanol, and dried at room temperature.

*General procedure for preparing thiazole-2(3H)-thiones*

A mixture of primary amine (1.0 mmol) and $CS_2$ (1.0 mmol) in ethanol (8 mL) was stirred for 5 min and then 2-bromoacetophenone or 2-bromo-1-(4-methoxyphenyl)ethanone (1.0 mmol) and $H_3PW_{12}O_{40}$-amino-functionalized $CdFe_{12}O_{19}@SiO_2$ nanocomposites (4 mg) were added, and the mixture was stirred for the appropriate times, as determined by TLC (*n*-hexane/ethyl acetate 7:3). After the completion of the reaction, the nanocomposite was separated from the reaction before working up by an external magnet field. The solid rinsed with EtOH to get a pure product. All of the compounds were identified on the basis of their $^1$H NMR, $^{13}$C NMR, FT-IR, and elemental analyses, all of which were submitted in the supporting information.

*3-Benzyl-4-phenyl-1,3-thiazole-2(3H)-thione* (**4a**):

Colorless viscous oil; FT-IR (KBr): 3103, 3004, 1605, 1476, 1203 cm$^{-1}$; $^1$H NMR (250 MHz, $CDCl_3$): $\delta$ 4.91 (s, 2H, $CH_2$), 6.04 (s, 1H, CH of alkene), 6.94–7.35 (m, 10H, CH, ArH). $^{13}$C NMR (62.5 MHz, $CDCl_3$): $\delta$ 47.25, 98.85, 127.05, 127.45, 128.50, 128.55, 129.05, 133.30, 137.45, 154.85, 178.35, 197.20. Anal. Calcd. for $C_{16}H_{13}NS_2$ (283): C, 67.81; H, 4.62; N, 4.94. Found: C, 67.71; H, 4.53; N, 4.74 %.

*Determination of antimicrobial activity*

The antimicrobial activity of compounds is determined using Agar diffusion [35]. Streptomycin (10µg/well) as a standard drug was applied as a positive control for bacteria, and Nystatine (100 IU/well) was used for fungi; DMSO was used as a negative control. The results were considered for each tested compound as the average diameter of inhibition zones of bacterial and fungal around the wells in mm.

## RESULTS AND DISCUSSION

The particle size and morphology of $H_3PW_{12}O_{40}$-amino-functionalized $CdFe_{12}O_{19}@SiO_2$ nanocomposites was considered by SEM which clearly revealed that the average size of the particles is about 80 nanometers (Figure 1).

Figure 2 indicates the powder X-ray diffraction (XRD) pattern of $H_3PW_{12}O_{40}$-amino-functionalized $CdFe_{12}O_{19}@SiO_2$ nanocomposites. The pattern agrees correctly with the presented pattern for $CdFe_{12}O_{19}$ [33-34]. The crystallite size of the nanocatalyst calculated by the Debye–Scherer equation is about 84-86 nm.

Figure 3 shows the FT-IR spectra of $CdFe_{12}O_{19}$, $CdFe_{12}O_{19}@SiO_2$, amino-functionalized $CdFe_{12}O_{19}@SiO_2$ and $H_3PW_{12}O_{40}$-amino-functionalized $CdFe_{12}O_{19}@SiO_2$ nanocomposites. The FT-IR spectra of $CdFe_{12}O_{19}$ display the vibrations of the metal–oxygen stretching at 555-565 cm$^{-1}$. The absorption peak at 3436 cm$^{-1}$ is corresponded to the stretching vibrational absorptions of O-H. The bands at 467, 1078, 1636, and 3425 cm$^{-1}$ are the characteristic absorptions of $SiO_2$, which provides the evidence for the formation of a silica shell. The

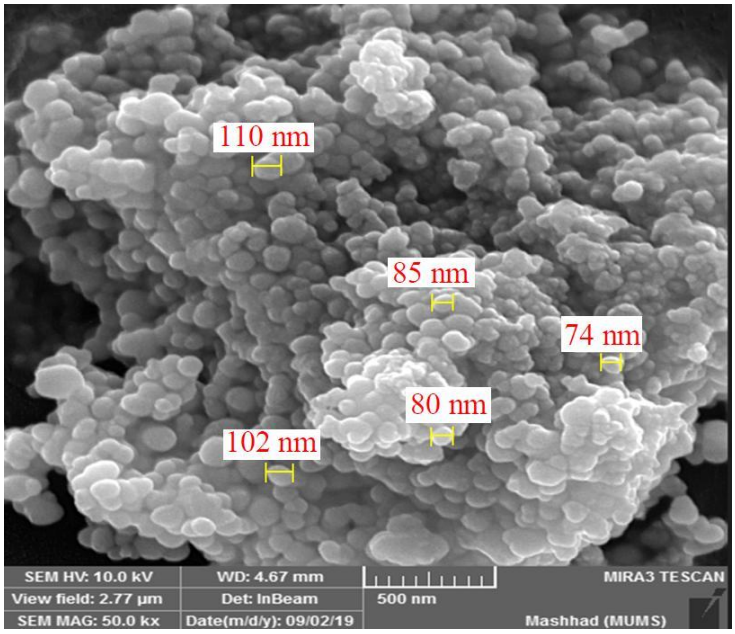


Fig. 1. SEM of $H_3PW_{12}O_{40}$ -amino-functionalized $CdFe_{12}O_{19}@SiO_2$

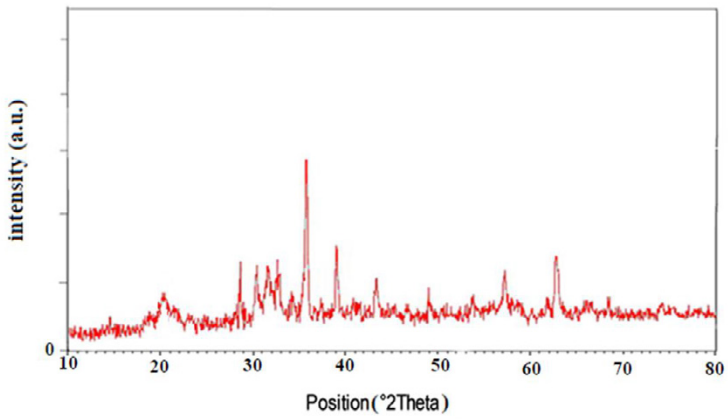


Fig 2. The XRD of $H_3PW_{12}O_{40}$ -amino-functionalized $CdFe_{12}O_{19}@SiO_2$

increase of the bands at 1572 $cm^{-1}$ is a direct indication of the existence of the N-H bending vibration (Fig. 3c). The bands at 1080, 980, 880, and 773 $cm^{-1}$, which are the fingerprint of the Keggin structure of $H_3PW_{12}O_{40}$, are usually corresponded to P-O, W=O, W-O-W in corner shared octahedral, and W- O-W in edge shared octahedral [36-37] (Fig. 3d).

The magnetic attributes of $CdFe_{12}O_{19}$ (b), $CdFe_{12}O_{19}@SiO_2$ (c), amino-functionalized $CdFe_{12}O_{19}$ $@SiO_2$ (d), and $H_3PW_{12}O_{40}$-amino-functionalized $CdFe_{12}O_{19}@SiO_2$ nanocomposites were measured with VSM (Figure 4). The amounts of saturation-magnetization for $CdFe_{12}O_{19}$ and $H_3PW_{12}O_{40}$-amino-functionalized $CdFe_{12}O_{19}@SiO_2$ nanocomposites are 12.80 and 1.98 emu/g, respectively. These results demonstrate that the magnetization properties are lessened using the coating. Furthermore, these results also indicate that the $H_3PW_{12}O_{40}$ -amino-functionalized $CdFe_{12}O_{19}@SiO_2$ nanocatalyst remains magnetic after coating. This is advantageous because magnetic nanocatalyst can be easily collected from the reaction media by an external magnet field over a short period of time.

Thermogravimetric analysis (TGA) peruses

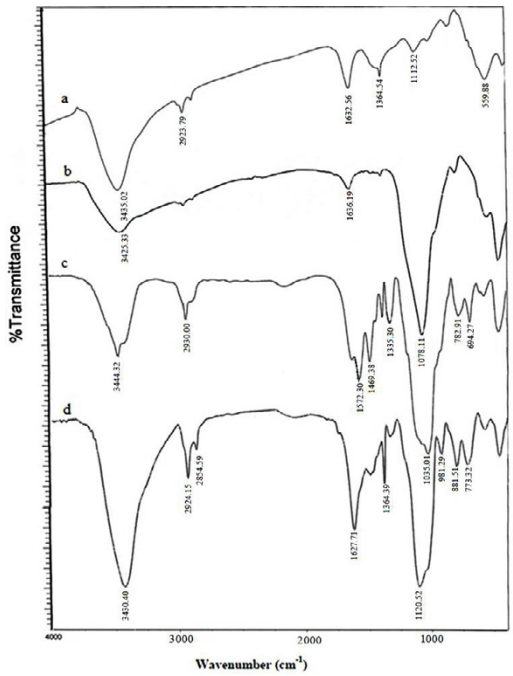


Fig 3. FT-IR of (a) $CdFe_{12}O_{19}$ (b) $CdFe_{12}O_{19}@SiO_2$ (c) Amino-functionalized $CdFe_{12}O_{19}@SiO_2$ (d) $H_3PW_{12}O_{40}$-amino-functionalized $CdFe_{12}O_{19}@SiO_2$

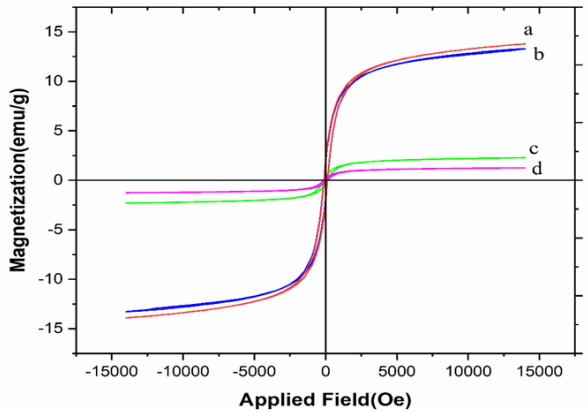


Fig. 4. The VSM curve of: (a) $CdFe_{12}O_{19}$ (b) $CdFe_{12}O_{19}@SiO_2$ (c) Amino-functionalized $CdFe_{12}O_{19}@SiO_2$ (d) $H_3PW_{12}O_{40}$-amino-functionalized $CdFe_{12}O_{19}@SiO_2$

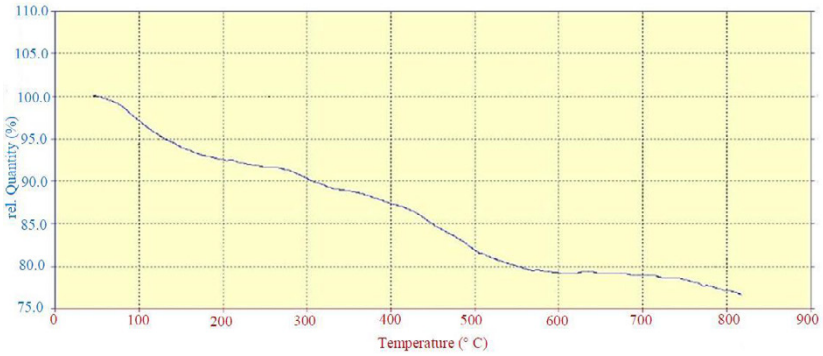


Fig. 5. TGA curve of $H_3PW_{12}O_{40}$-amino-functionalized $CdFe_{12}O_{19}@SiO_2$

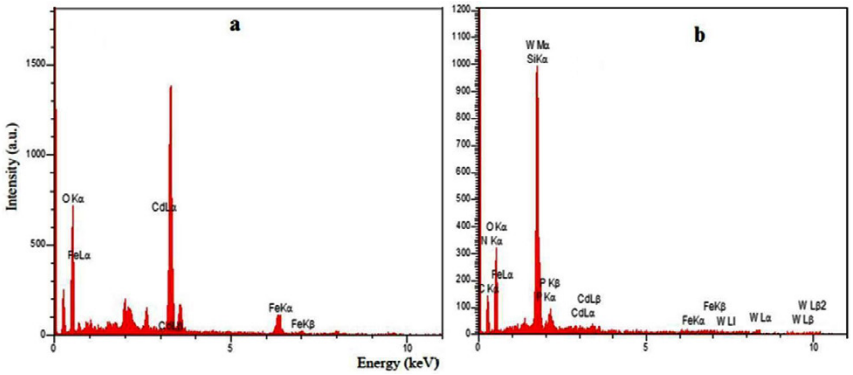


Fig. 6. EDS of (a) $CdFe_{12}O_{19}$ (b) $H_3PW_{12}O_{40}$ -amino-functionalized $CdFe_{12}O_{19}$@$SiO_2$

Table 1. Optimization of reaction conditions [a]

| Entry | Solvent | Catalyst | Time (h) | Yield (%)[b] |
|---|---|---|---|---|
| 1 | EtOH | — | 8 | 15 |
| 2 | EtOH | CAN (8 mg) | 6 | 42 |
| 3 | EtOH | $NaHSO_4$ (10 mg) | 6 | 35 |
| 4 | EtOH | $CdFe_{12}O_{19}$ (6 mg) | 6 | 40 |
| 5 | EtOH | $CdFe_{12}O_{19}$@$SiO_2$ (6 mg) | 3 | 64 |
| 6 | EtOH | amino-functionalized $CdFe_{12}O_{19}$ @$SiO_2$ (6 mg) | 3 | 62 |
| 7 | $H_2O$ | $H_3PW_{12}O_{40}$-amino-functionalized $CdFe_{12}O_{19}$@$SiO_2$ nanocomposite (4 mg) | 3 | 50 |
| 8 | DMF | $H_3PW_{12}O_{40}$-amino-functionalized $CdFe_{12}O_{19}$@$SiO_2$ nanocomposite (4 mg) | 3 | 63 |
| 9 | $CH_3CN$ | $H_3PW_{12}O_{40}$-amino-functionalized $CdFe_{12}O_{19}$@$SiO_2$ nanocomposite (4 mg) | 2.5 | 76 |
| 10 | EtOH | $H_3PW_{12}O_{40}$-amino-functionalized $CdFe_{12}O_{19}$@$SiO_2$ nanocomposite (3 mg) | 2.5 | 90 |
| 11 | EtOH | $H_3PW_{12}O_{40}$-amino-functionalized $CdFe_{12}O_{19}$@$SiO_2$ nanocomposite (4 mg) | 2.5 | 94 |
| 12 | EtOH | $H_3PW_{12}O_{40}$-amino-functionalized $CdFe_{12}O_{19}$@$SiO_2$ nanocomposite (5 mg) | 2.5 | 94 |

[a] 2-bromoacetophenone (1 mmol), $CS_2$ (1 mmol) and benzyl amine (1 mmol) [b]Isolated yield

Table 2. Synthesis of thiazole-2(3H)-thiones using $H_3PW_{12}O_{40}$-amino-functionalized $CdFe_{12}O_{19}$@$SiO_2$ nanocomposite (4 mg)

| Product | R | Ar | Time (h) | Yield[a] |
|---|---|---|---|---|
| **4a** | $PhCH_2$ | Ph | 2.5 | 94% |
| **4b** | 3,4-$Cl_2PhCH_2$ | Ph | 3 | 86% |
| **4c** | $PhC_4H_3CH_2$ | Ph | 3 | 85% |
| **4d** | furanyl-$CH_2$ | Ph | 2.5 | 85% |
| **4e** | 4-$FPhCH_2$ | Ph | 2.5 | 88% |
| **4f** | 2-OMe-$PhCH_2$ | Ph | 2.5 | 92% |
| **4g** | 4-Me-$PhCH_2$ | 4-OMe-Ph | 2.5 | 87% |
| **4h** | $PhCH_2$ | 4-OMe-Ph | 3 | 81% |
| **4i** | furanyl-$CH_2$ | 4-OMe-Ph | 3 | 79% |
| **4j** | 2-OMe-$PhCH_2$ | 4-OMe-Ph | 3 | 84% |

[a] Isolated yield

the thermal stability of the $H_3PW_{12}O_{40}$-amino-functionalized $CdFe_{12}O_{19}$@$SiO_2$ nanocomposites. The weight loss at temperatures below 200 °C is due to the removal of physically adsorbed solvent and surface hydroxyl groups. The curve exhibited a weight loss of about 12 % from 220 to 600 °C owing to the decomposition of the organic spacer grafting to the nanocomposite surface (Figure 5).

The energy-dispersive X-ray spectrum (EDS) of $H_3PW_{12}O_{40}$-amino-functionalized $CdFe_{12}O_{19}$@$SiO_2$ nanocomposites (Figure 6) displays that the elemental compositions are carbon, cadmium, oxygen, iron, tungsten, silicon, nitrogen, and phosphorus.

We used the reaction of $CS_2$, 2-bromoacetophenone and benzyl amine on 1 mmol scale as a model

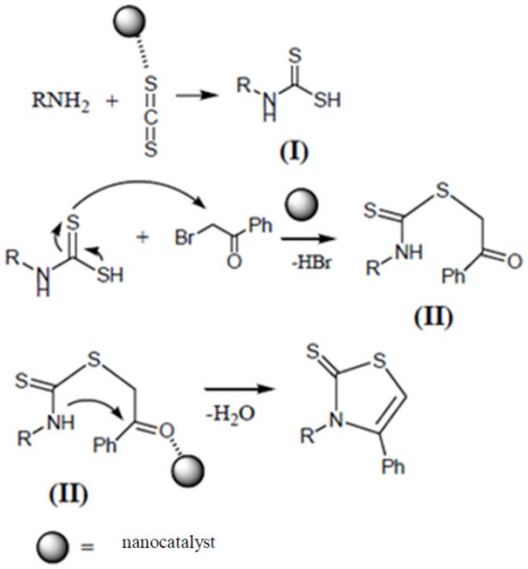


Scheme 3. A proposed mechanism for the synthesis of thiazoles

Table 3. In vitro antimicrobial activity of the compounds using agar diffusion assay

| Test microorganisms | Diameter of zone of inhibition in mm | | | | | | | | | | | |
|---|---|---|---|---|---|---|---|---|---|---|---|---|
| | **4a** | **4b** | **4c** | **4d** | **4e** | **4f** | **4g** | **4h** | **4i** | **4j** | **Streptomycin** | **Nystatin** |
| P. aeruginosa | * | 11 | * | * | 10 | * | * | * | * | * | 22 | NT |
| E. coli | * | * | * | * | * | 11 | * | * | * | 12 | 25 | NT |
| K. pneumonia | * | 10 | * | * | * | * | * | * | * | * | 24 | NT |
| S. dysenteriae | * | 10 | * | * | * | * | * | * | * | * | 24 | NT |
| P. vulgaris | * | * | * | * | * | * | * | * | * | * | 23 | NT |
| S. paratyphi-A | * | * | * | * | * | * | * | * | * | * | 28 | NT |
| B. subtilis | * | 16 | * | * | 13 | 12 | * | * | * | 12 | 25 | NT |
| S. aureus | * | 17 | * | * | 12 | 10 | * | * | * | 11 | 28 | NT |
| S. epidermidis | * | 12 | * | * | 10 | 10 | * | * | * | 11 | 22 | NT |
| C. albicans | * | 12 | * | * | * | * | * | * | * | * | NT | 25 |
| A. niger | * | 16 | * | * | * | * | * | * | * | * | NT | 32 |
| A. brasiliensis | * | 14 | * | * | * | * | * | * | * | * | NT | 33 |

*Not Active.
NT: not tested.

reaction and carried it out using CAN, $NaHSO_4$, $CdFe_{12}O_{19}$, $CdFe_{12}O_{19}@SiO_2$, amino-functionalized $CdFe_{12}O_{19}@SiO_2$ and $H_3PW_{12}O_{40}$-amino-functionalized $CdFe_{12}O_{19}@SiO_2$ nanocomposite. We found that the reaction gave useful results using $H_3PW_{12}O_{40}$-amino-functionalized $CdFe_{12}O_{19}@SiO_2$ nanocomposite (4 mg) (Table 1). The best results were exemplified in Entry 11 with 94% yield. Further, we also reacted 2-bromoacetophenone or 2-bromo-1-(4-methoxyphenyl)ethanone with $CS_2$ and other primary amines and uniformly found satisfactory results (Table 2, mean 86%). The yield did not appear to be exclusively sensitive to the substituent groups. The structures of the products were deduced from their $^1$H NMR, $^{13}$C NMR, and FT-IR.

The reusability of $H_3PW_{12}O_{40}$-amino-functionalized $CdFe_{12}O_{19}@SiO_2$ nanocomposite (4 mg) was considered for the model reaction, and it was found that product yields lessened only to a very small extent on each reuse (run 1, 94%; run 2, 94%; run 3, 93%; run 4, 93%; run 5, 92%; run 6, 92%). After the completion of the reaction, the nanocatalyst was separated by an external magnet. The catalyst was rinsed four times with ethanol and dried at room temperature for 10 h.

Scheme 3 displays a proposed mechanism for

this reaction in the presence of $H_3PW_{12}O_{40}$-amino-functionalized $CdFe_{12}O_{19}@SiO_2$ nanocomposite as catalyst. Initially, the nucleophilic attack by amines on a carbon disulfide generates intermediate (I); the next step involves the nucleophilic attack of intermediate (I) on the methylene carbon of phenacyl bromide, leading to intermediate (II); then, ring closure was achieved by intramolecular attack of nitrogen at the carbonyl carbon to afford the 3-alkyl-4-phenyl-1,3- thiazole-2(3*H*)-thione derivatives. In this mechanism the surface atoms of $H_3PW_{12}O_{40}$-amino-functionalized $CdFe_{12}O_{19}@SiO_2$ nanocomposite activate the C=S and C=O groups for better reaction with nucleophiles.

The antimicrobial activity of compounds is determined using Agar diffusion [35]. The results are exhibited in Table 3. The compounds **4b**, **4e**, **4f**, and **4j** have moderate growth inhibitory effects on Gram positive bacteria (*Staphylococcus aureus, Bacillus subtilis*; and *Staphylococcus epidermidis*). The compound **4b** has moderate growth inhibitory effects on fungi.

## CONCLUSIONS

In conclusion, we demonstrated an efficient way for the preparation of thiazole-2(3H)-thiones by three-component reactions of $CS_2$, 2-bromoacetophenone or 2-bromo-1-(4-methoxyphenyl)ethenone, and a primary amine using $H_3PW_{12}O_{40}$-amino-functionalized $CdFe_{12}O_{19}@SiO_2$ nanocomposites in ethanol. The compounds **4b**, **4e**, **4f,** and **4j** have moderate growth inhibitory effects on Gram positive bacteria (*Staphylococcus aureus, Bacillus subtilis*; and *Staphylococcus epidermidis*). The compound **4b** has moderate growth inhibitory effects on fungi. This protocol has a number of salient features including great yields in concise times, retrievability of the nanocatalyst, little nanocatalyst loading, and antibacterial activities for four compounds.

## REFERENCES


[1] Dawood KM, Gomha SM. Synthesis and Anti-cancer Activity of 1,3,4-Thiadiazole and 1,3-Thiazole Derivatives Having 1,3,4-Oxadiazole Moiety. Journal of Heterocyclic Chemistry. 2015;52(5):1400-5.

[2] Abdel-Wahab BF, Abdel-Aziz HA, Ahmed EM. Synthesis and antimicrobial evaluation of some 1,3-thiazole, 1,3,4-thiadiazole, 1,2,4-triazole, and 1,2,4-triazolo[3,4-b][1,3,4]-thiadiazine derivatives including a 5-(benzofuran-2-yl)-1-phenylpyrazole moiety. Monatshefte für Chemie - Chemical Monthly. 2009;140(6):601-5.

[3] Sharma RN, Xavier FP, Vasu KK, Chaturvedi SC, Pancholi SS. Synthesis of 4-benzyl-1,3-thiazole derivatives as potential anti-inflammatory agents: An analogue-based drug design approach. Journal of Enzyme Inhibition and Medicinal Chemistry. 2009;24(3):890-7.

[4] Maillard LT, Bertout S, Quinonéro O, Akalin G, Turan-Zitouni G, Fulcrand P, et al. Synthesis and anti-Candida activity of novel 2-hydrazino-1,3-thiazole derivatives. Bioorganic & Medicinal Chemistry Letters. 2013;23(6):1803-7.

[5] Holla BS, Malini KV, Rao BS, Sarojini BK, Kumari NS. Synthesis of some new 2,4-disubstituted thiazoles as possible antibacterial and anti-inflammatory agents. European Journal of Medicinal Chemistry. 2003;38(3):313-8.

[6] Wilson SM, Wurst MG, Whatley MF, Daniels RN. Classics in Chemical Neuroscience: Pramipexole. ACS Chemical Neuroscience. 2020;11(17):2506-12.

[7] Kojić V, Popsavin M, Spaić S, Jakimov D, Kovačević I, Svirčev M, et al. Structure based design, synthesis and in vitro antitumour activity of tiazofurin stereoisomers with nitrogen functions at the C-2′ or C-3′ positions. European Journal of Medicinal Chemistry. 2019;183:111712.

[8] Zhu Z, Lu Z, Xu T, Chen C, Yang G, Zha T, et al. Arbidol monotherapy is superior to lopinavir/ritonavir in treating COVID-19. Journal of Infection. 2020;81(1):e21-e3.

[9] Basit AW, Newton JM, Lacey LF. Susceptibility of the H2-receptor antagonists cimetidine, famotidine and nizatidine, to metabolism by the gastrointestinal microflora. International Journal of Pharmaceutics. 2002;237(1):23-33.

[10] Masquelin T, Obrecht D. A new general three component solution-phase synthesis of 2-amino-1,3-thiazole and 2,4-diamino-1,3-thiazole combinatorial libraries. Tetrahedron. 2001;57(1):153-6.

[11] Kumar D, Sonawane M, Pujala B, Jain VK, Bhagat S, Chakraborti AK. Supported protic acid-catalyzed synthesis of 2,3-disubstituted thiazolidin-4-ones: enhancement of the catalytic potential of protic acid by adsorption on solid supports. Green Chemistry. 2013;15(10):2872-84.

[12] Foroughifar N, Ebrahimi S. One-pot synthesis of 1,3-thiazolidin-4-one using Bi(SCH2COOH)3 as catalyst. Chinese Chemical Letters. 2013;24(5):389-91.

[13] Subhedar DD, Shaikh MH, Arkile MA, Yeware A, Sarkar D, Shingate BB. Facile synthesis of 1,3-thiazolidin-4-ones as antitubercular agents. Bioorganic & Medicinal Chemistry Letters. 2016;26(7):1704-8.

[14] Su W, Liu C, Shan W. Ytterbium (III) triflate catalyzed one-pot synthesis of 1, 3-thiazolidin-2-imines from epichlorohydrin and thioureas. Synlett. 2008;2008(05):725-7.

[15] Azizi S, Soleymani J, Hasanzadeh M. KCC-1/Pr-SO3H: an efficient heterogeneous catalyst for green and one-pot synthesis of 2,3-dihydroquinazolin-4(1H)-one. Nanocomposites. 2020;6(1):31-40.

[16] Azizi S, Shadjou N, Hasanzadeh M. KCC-1-NH2-DPA: an efficient heterogeneous recyclable nanocomposite for the catalytic synthesis of tetrahydrodipyrazolopyridines as a well-known organic scaffold in various bioactive derivatives. Nanocomposites. 2019;5(4):124-32.

[17] Shokouhimehr M, Piao Y, Kim J, Jang Y, Hyeon T. A magnetically recyclable nanocomposite catalyst for olefin epoxidation. Angewandte Chemie. 2007;119(37):7169-73.

[18] Zhang J, Wang Y, Ji H, Wei Y, Wu N, Zuo B, et al. Magnetic nanocomposite catalysts with high activity and selectivity for selective hydrogenation of ortho-chloronitrobenzene.

Journal of Catalysis. 2005;229(1):114-8.
[19] Shahbazi-Alavi H, Teymuri R, Safaei-Ghomi J. HPA-ZSM-5 nanocomposite as a highly effective and easily retrievable catalyst for the synthesis of furans. Nanochemistry Research. 2021;6(2):135-42.
[20] Shahbazi-Alavi H, Ebrahimi SM, Safaei-Ghomi J. CuO/ZnO@ N-GQDs@ NH2 nanocomposite as superior catalyst for the synthesis of pyrimidine-triones. Nanochemistry Research. 2021;6(1):10-7.
[21] Rostami Z, Rouhanizadeh M, Nami N, Zareyee D, Fe3O4 magnetic nanoparticles (MNPs) as an effective catalyst for synthesis of indole derivatives, 2018;3:142-148.
[22] Nami N, Zareyee D, Ghasemi M, Asgharzadeh A, Forouzani M, Mirzad S, et al. An efficient method for synthesis of some heterocyclic compounds containing 3-iminoisatin and 1,2,4-triazole using Fe3O4 magnetic nanoparticles. Journal of Sulfur Chemistry. 2017;38(3):279-90.
[23] Heidarzadeh T, Nami N, Zareyee D, editors. Synthesis of Indole Derivatives Using Biosynthesized ZnO-CaO Nanoparticles as an Efficient Catalyst. Journal of Nano Research; 2021: Trans Tech Publ.
[24] Safaei-Ghomi J, Aghagoli R, Shahbazi-Alavi H. Synthesis of hexahydro-4-phenylquinoline-3-carbonitriles using Fe3O4@SiO2-SO3H nanoparticles as a superior and retrievable heterogeneous catalyst under ultrasonic irradiations. Zeitschrift für Naturforschung B. 2018;73(5):269-74.
[25] Safaei-Ghomi J, Lashkari MR, Shahbazi-Alavi H. Synthesis of bis-spiropiperidines using nano-CuFe2O4@chitosan as a robust and retrievable heterogeneous catalyst. Journal of Chemical Research. 2017;41(7):416-9.
[26] Hedayatnasab Z, Abnisa F, Daud WMAW. Review on magnetic nanoparticles for magnetic nanofluid hyperthermia application. Materials & Design. 2017;123:174-96.
[27] Sharma RK, Dutta S, Sharma S, Zboril R, Varma RS, Gawande MB. Fe3O4 (iron oxide)-supported nanocatalysts: synthesis, characterization and applications in coupling reactions. Green Chemistry. 2016;18(11):3184-209.
[28] Dalpozzo R. Magnetic nanoparticle supports for asymmetric catalysts. Green Chemistry. 2015;17(7):3671-86.
[29] Shahbazi-Alavi H, Khojasteh-Khosro S, Safaei-Ghomi J, Tavazo M. Crosslinked sulfonated polyacrylamide (Cross-PAA-SO3H) tethered to nano-Fe3O4 as a superior catalyst for the synthesis of 1,3-thiazoles. BMC Chemistry. 2019;13(1):120.
[30] Safaei-Ghomi J, Tavazo M, Shahbazi-Alavi H. Chitosan-attached nano-Fe3O4 as a superior and retrievable heterogeneous catalyst for the synthesis of benzopyranophenazines using chitosan-attached nano-Fe3O4. Zeitschrift für Naturforschung B. 2019;74(10):733-8.
[31] Schnee J, Gaigneaux EM. Lifetime of the H3PW12O40 heteropolyacid in the methanol-to-DME process: A question of pre-treatment. Applied Catalysis A: General. 2017;538:174-80.
[32] Micek-Ilnicka A, Bielańska E, Lityńska-Dobrzyńska L, Bielański A. Carbon nanotubes, silica and titania supported heteropolyacid H3PW12O40 as the catalyst for ethanol conversion. Applied Catalysis A: General. 2012;421-422:91-8.
[33] Mahdiani M, Sobhani A, Salavati-Niasari M. The first synthesis of CdFe12O19 nanostructures and nanocomposites and considering of magnetic, optical, electrochemical and photocatalytic properties. Journal of Hazardous Materials. 2019;367:607-19.
[34] Mahdiani M, Soofivand F, Ansari F, Salavati-Niasari M. Grafting of CuFe12O19 nanoparticles on CNT and graphene: Eco-friendly synthesis, characterization and photocatalytic activity. Journal of Cleaner Production. 2018;176:1185-97.
[35] Safaei-Ghomi J, Paymard-Samani S, Zahraie Z, Shahbazi-Alavi H. Synthesis of 1,5 and 2,5-disubstituted tetrazoles using NiO nanoparticles and their evaluation as antimicrobial agents. Nanomedicine Research Journal. 2019;4(2):91-100.
[36] Rocchiccioli-Deltcheff C, Fournier M, Franck R, Thouvenot R. Vibrational investigations of polyoxometalates. 2. Evidence for anion-anion interactions in molybdenum(VI) and tungsten(VI) compounds related to the Keggin structure. Inorganic Chemistry. 1983;22(2):207-16.
[37] Yang L, Qi Y, Yuan X, Shen J, Kim J. Direct synthesis, characterization and catalytic application of SBA-15 containing heteropolyacid H3PW12O40. Journal of Molecular Catalysis A: Chemical. 2005;229(1):199-205.